Energetics of the Li amide/Li imide hydrogen storage reaction

J. F. Herbst and L. G. Hector, Jr.
Materials and Processes Laboratory, General Motors R&D Center, Warren, Michigan 48090-9055, USA
(Received 11 January 2005; revised manuscript received 1 July 2005; published 22 September 2005)

A density functional theory investigation of the recently identified hydrogen storage reaction $LiNH_2 + LiH \leftrightarrow Li_2NH + H_2$ is described. The electronic structure and enthalpy of formation ΔH of each constituent are calculated in both the generalized gradient approximation (GGA) and the local density approximation (LDA). Zero point energies and finite temperature corrections to ΔH are derived via calculation of the vibrational spectra. We find that the GGA provides much more favorable agreement with experiment than the LDA for the structural parameters and for $\Delta H(LiNH_2)$, $\Delta H(LiH)$, and the overall reaction enthalpy.

DOI: 10.1103/PhysRevB.72.125120 PACS number(s): 71.20.−b

I. INTRODUCTION

Recent investigation of the reaction of Li_3N with H_2 gas by Chen *et al.*,[1] extending much earlier work,[2,3] has led to the identification of the reversible reaction

$$LiNH_2 + LiH \leftrightarrow Li_2NH + H_2 \quad (1)$$

as a potential mechanism for hydrogen storage.[1,4–6] This pathway is intriguing since it involves reaction of two stable compounds (lithium amide, $LiNH_2$, and LiH) to yield another stable compound (lithium imide, Li_2NH) and H_2 gas, rather than release of H_2 from a single parent phase. H_2 production initiates at ~150 °C, lower than for either $LiNH_2$ (~200 °C) or LiH (~550 °C) alone,[4] and the theoretical 6.5 mass % H_2 capacity is substantial. Understanding the energetics of reactions such as (1) is of fundamental interest for solid state physics; moreover, it will buttress the discovery and design of material systems having specific hydrogen storage characteristics. In particular, the enthalpies of formation ΔH of the compounds are vital since they determine the overall reaction enthalpy ΔH_R and thus control the equilibrium H_2 pressure p and temperature T via the van't Hoff relation[7]

$$\ln p/p_0 = \Delta H_R/RT - \Delta S_R/R, \quad (2)$$

where ΔS_R is the corresponding entropy change (largely due to H_2), p_0 is unit H_2 pressure, and R is the gas constant.

Here we describe calculations of the electronic structure, phonon spectra, and ΔH by means of density functional theory (DFT) using both the local density approximation (LDA) and the generalized gradient approximation (GGA) for the exchange-correlation energy functional μ_{xc}. We report $T=0$ and $T=298$ K values of ΔH that, respectively, include zero point energies and finite temperature corrections derived from the vibrational spectra. The choice of μ_{xc} has profound impact on the results. The GGA affords substantially better agreement with experiment than the LDA for the crystal structure parameters of $LiNH_2$, LiH, Li_2NH and for $\Delta H(LiNH_2)$, $\Delta H(LiH)$, and ΔH_R. Our findings point to a need for more accurate measurements of $\Delta H(Li_2NH)$.

II. CALCULATIONAL PROCEDURES

Electronic total energies were calculated with the Vienna *ab initio* simulation package (VASP), which implements DFT[8] using a plane wave basis set.[9,10] Projector-augmented wave potentials[11] were employed for the elemental constituents; the H, Li, and N potentials contained one, three, and five valence electrons, respectively. The LDA and GGA calculations were performed with the Ceperley-Alder[12] and Perdew-Wang[13,14] versions of μ_{xc}, respectively.

The crystal structures of $LiNH_2$ and LiH are known, the hydrogen positions having been determined accurately by the traditional means of neutron diffraction on the corresponding deuterides;[15,16] Table I lists the structural parameters. There is disagreement in the extant literature, however, regarding the structure of Li_2NH. An antifluorite structure (fcc $Fm\bar{3}m$ space group, No. 225) was suggested in the early 1950s, but the H sites were not identified.[19] Recently, Noritake *et al.*[20] proposed, on the basis of x-ray powder diffraction work on Li_2NH, that the hydrogens randomly occupy 12 of the 48*h* sites in the antifluorite structure. In contrast, Ohoyama *et al.*[21] concluded from neutron powder diffraction (NPD) measurements on Li_2NH that the structure is fcc but in the $F\bar{4}3m$ (No. 216) space group, with four hydrogens randomized over the 16*e* sites. To clarify the situation Balogh *et al.*[22] have conducted NPD experiments on a deuterated sample. Their measurements in the 100 K–300 K interval demonstrate the existence of a single low temperature phase that can be described to the same degree of accuracy as a disordered cubic or a fully occupied orthorhombic structure. (Balogh *et al.*[22] also show that the disordered models of Noritake *et al.*[20] and Ohoyama *et al.*[21] are equivalent, in the sense of identical powder diffraction patterns, to lower symmetry, fully occupied orthorhombic and rhombohedral structures, respectively.) In our opinion this is the best available structure for Li_2NH, and we have no doubt that the enthalpy of formation ΔH we derive for it (Sec. III D) is as accurate as those we obtain for $LiNH_2$ and LiH. We use the orthorhombic representation since it facilitates our DFT efforts by obviating uncertainties associated with treating partially occupied sites in large unit cells. Figure 1 illustrates the structure. The Li_2NH groups in the solid are planar, as are the free imide and amide molecules;[23] however, the $LiNH_2$ complexes in the solid amide are tetrahedral.

TABLE I. Crystal structure parameters for $LiNH_2$ amide (tetragonal $I\bar{4}$ structure; space group No. 82), LiH (fcc $Fm\bar{3}m$; No. 225), Li metal (bcc $Im\bar{3}m$; No. 229), and internuclear distances d(N-N) and d(H-H) for the N_2 and H_2 molecules. Experimental information from Refs. 15 and 16 for $LiNH_2$; Ref. 17 for LiH; Ref. 15 for Li; Ref. 18 for N_2 and H_2.

			Calc		
			LDA	GGA	Expt.
$LiNH_2$					
	a (Å)		4.763	5.017	5.037
	c (Å)		10.061	10.363	10.278
	Li ($4f$)	z	0.0092	0.0062	0.0042
	N ($8g$)	x	0.2387	0.2306	0.2284
		y	0.2439	0.2459	0.2452
		z	0.1181	0.1156	0.1148
	H ($8g_1$)	x	0.2316	0.2299	0.235
		y	0.0951	0.1157	0.113
		z	0.1928	0.1921	0.186
	H ($8g_2$)	x	0.4383	0.4131	0.389
		y	0.3257	0.3362	0.362
		z	0.1269	0.1241	0.120
LiH	a (Å)		3.912	3.998	4.066
Li	a (Å)		3.362	3.426	3.510
N_2	d(N-N) (Å)		1.0948	1.1009	1.0976
H_2	d(H-H) (Å)		0.7659	0.7489	0.7461

At least two simultaneous relaxations of the lattice constants and nuclear coordinates of each structure were conducted by minimizing the Hellman-Feynman forces via a conjugate gradient method. Final total energies were calculated using the linear tetrahedron method with Blöchl corrections[24] on the relaxed structures. The plane wave cutoff energy was at least 900 eV for the solids and molecules, and in all cases the total energy was converged to 10^{-6} eV/cell and the force components relaxed to at least 10^{-4} eV/Å. k meshes having 186, 280, 64, and 190 points in the irreducible Brillouin zones of $LiNH_2$, LiH, Li_2NH, and Li metal (calculations for which are needed to derive ΔH for the Li-containing materials), respectively, were utilized. The energies of the free H_2 and N_2 molecules were computed with the same potentials via VASP calculations in a $11 \times 12 \times 13$ Å^3 cell. This was sufficient to converge the energies of the isolated dimers without interaction effects from periodic images.

Phonon spectra for the solids and the vibrational frequency of H_2 and N_2 were computed with the direct method.[25,26] For the solids this involves construction of one unperturbed and N perturbed supercells, where N is the number of degrees of freedom of the atomic positions as restricted by the symmetry of the system. In each perturbed supercell, a single atom is displaced in a Cartesian direction in such a way that the N supercells explore all of the degrees of freedom of each symmetry-unique atomic site. The Hellman-Feynman forces on all atoms are computed with VASP. Each supercell was made large enough to ensure that the interactions between equivalent atoms in periodic images and the computed force constants at the boundaries are negligible. We constructed the supercells from the VASP-optimized GGA and LDA structures and used ±0.01 Å atomic displacements in all cases (test calculations with smaller displacements showed no changes in the results). For the amide we employed (2 2 1) supercells (128 atoms), 33 distinct versions of which were required. To ensure that the structure was adequately explored for possible soft modes we also investigated 33 64-atom (1 1 2) supercells. For the imide we conducted calculations on 73 different 256-atom (2 1 2) and 73 distinct 128-atom (1 2 1) supercells. For LiH we chose (2 2 2) supercells containing 64 atoms; the symmetry required calculations on five distinct supercells. For Li we conducted calculations on three distinct 250-atom (5 5 5) supercells. The dynamical matrix is derived from the force constants, which are computed through a least-squares fit to the

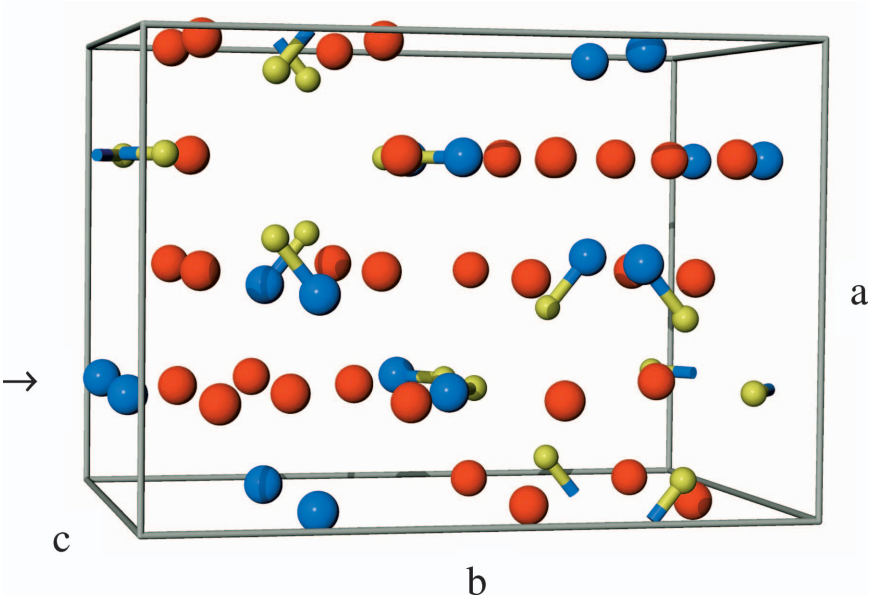

FIG. 1. (Color) Orthorhombic unit cell of solid lithium imide, Li_2NH (Li, red; N, blue; H, yellow). Table II contains the structural parameters. The arrow indicates the (100) plane at x=0.25 for which the electron localization function was computed in Fig. 8.

equation of motion of the lattice within the harmonic approximation. We did not account for longitudinal optical–transverse optical (LO–TO) zone center splittings; however, their neglect has negligible impact on the quantities (zero point and total phonon energies) entering the formation enthalpies we calculate since they are integrals over the entire Brillouin zone. No evidence for structural instability was found for any of the solids ($LiNH_2$, Li_2NH, LiH, and Li metal). The same computational machinery was used to extract the vibrational frequency of the H_2 and N_2 molecules.

III. RESULTS

A. Crystal structure parameters

Tables I and II list calculated and experimental structural parameters. It is clear that the GGA provides much better agreement with the measured lattice constants of $LiNH_2$, LiH, Li metal, and Li_2NH than the LDA. Among the GGA results the maximum deviation from experiment is 2.4% for a(Li), while the maximum LDA discrepancy is 5.4% for $a(LiNH_2)$. The general tendency for the LDA to overbind ions in solids is reflected by its underestimation of the lattice constants of all these materials.

As is the most frequent practice, the structural parameters in Tables I and II were determined by minimizing the electronic total energies E_{el}, by far the largest in the problem, and the 2.4% maximum disparity between the experimental lattice constants and the GGA results is acceptably small. We used these parameters in calculating phonon dispersion relations from which zero point energies E_{ZPE} and finite temperature phonon corrections for the formation enthalpies ΔH were derived (Sec. III D). In principle, however, E_{ZPE} should also be calculated as a function of volume V and $[E_{el}(V)+E_{ZPE}(V)]$ minimized to derive the zero temperature lattice constants. This may have some impact for materials containing a substantial fraction of light elements. To assess it we performed such calculations for LiH since (i) it has the highest hydrogen concentration of the solids of interest here; (ii) it is the most computationally tractable, although still very demanding because the phonon dispersion relations must be computed at each of a number of volumes; and (iii) a previous inquiry with which to compare exists.[27] Figure 2(a) displays E_{ZPE} computed in both the GGA and LDA for 12 different volumes bracketing the experimental volume V_{expt}. The two sets of values are in close proximity to each other and to those of Roma *et al.*,[27] who employed the LDA and linear response theory for the phonons. Total energies with and without $E_{ZPE}(V)$ are shown in Fig. 2(b). Without $E_{ZPE}(V)$ fits to those curves with the Murnaghan, Birch, or Vinet equations of state[28] yield the lattice constant $a=4.00$ Å (3.91 Å) in the GGA (LDA) appearing in Table I. Inclusion of $E_{ZPE}(V)$ leads to $a=4.09$ Å (4.00 Å) in the GGA (LDA). Roma *et al.*[27] obtained $a=3.96$ Å in their LDA calculations; we agree that the LDA even with $E_{ZPE}(V)$ fails to provide a highly accurate value of the lattice constant. Essentially all the discrepancy between the GGA result and the experimental value of 4.07 Å, however, is removed by including $E_{ZPE}(V)$. The total energies, on the other hand, are much less sensitive to $E_{ZPE}(V)$ in the following sense. The minimum value of $[E_{el}(V)+E_{ZPE}(V)]$ in Fig. 2(b) is −5.944 (−6.256) eV/LiH in the GGA (LDA). At the volume V_{el}^0 for which E_{el} is a minimum, however, we find $[E_{el}(V_{el}^0)+E_{ZPE}(V_{el}^0)]=-5.940$ (−6.252) eV/LiH in the GGA (LDA); we used these values in evaluating ΔH in Sec. III D. The corresponding differences are at most 0.004 eV =0.4 kJ/mole and have insignificant effect on the ΔH results, our central objective, which are on the order of 100 kJ/mole. Evaluation of the phonon spectra at V_{el}^0, rather than over a series of volumes, is sufficiently accurate for our purpose.

TABLE II. Structural parameters for Li_2NH imide (orthorhombic *Ima*2 structure; No. 46). The experimental data are for Li_2ND at 100 K (Ref. 22).

		Calc		
		LDA	GGA	Expt.
a (Å)		6.924	7.118	7.133
b (Å)		9.773	10.072	10.087
c (Å)		6.886	7.088	7.133
Li ($4b_1$)	y	0.3838	0.3826	0.3734
	z	0.3703	0.3703	0.3750
Li ($4b_2$)	y	0.8754	0.8765	0.8766
	z	0.3703	0.3703	0.3750
Li ($4b_3$)	y	0.1056	0.1058	0.1250
	z	0.3703	0.3705	0.3750
Li ($4b_4$)	y	0.2500	0.2498	0.2876
	z	0.1203	0.1206	0.0499
Li ($8c_1$)	x	0.5075	0.5074	0.4984
	y	0.1160	0.1155	0.1250
	z	0.1357	0.1372	0.1266
Li ($8c_2$)	x	0.5075	0.5073	0.4984
	y	0.3840	0.3844	0.3750
	z	0.1048	0.1034	0.1234
N ($4b_1$)	y	0.0082	0.0087	0.0082
	z	0.6110	0.6101	0.6086
N ($4b_2$)	y	0.0082	0.0089	0.0082
	z	0.1295	0.1305	0.1414
N ($8c$)	x	0.4698	0.4691	0.4836
	y	0.2420	0.2405	0.2418
	z	0.3703	0.3700	0.3750
H ($4b_1$)	y	0.5539	0.5505	0.5476
	z	0.2336	0.2295	0.2203
H ($4b_2$)	y	0.5539	0.5506	0.5476
	z	0.5070	0.5114	0.5297
H ($8c$)	x	0.5869	0.5819	0.5953
	y	0.1913	0.1945	0.2024
	z	0.8703	0.8700	0.8750

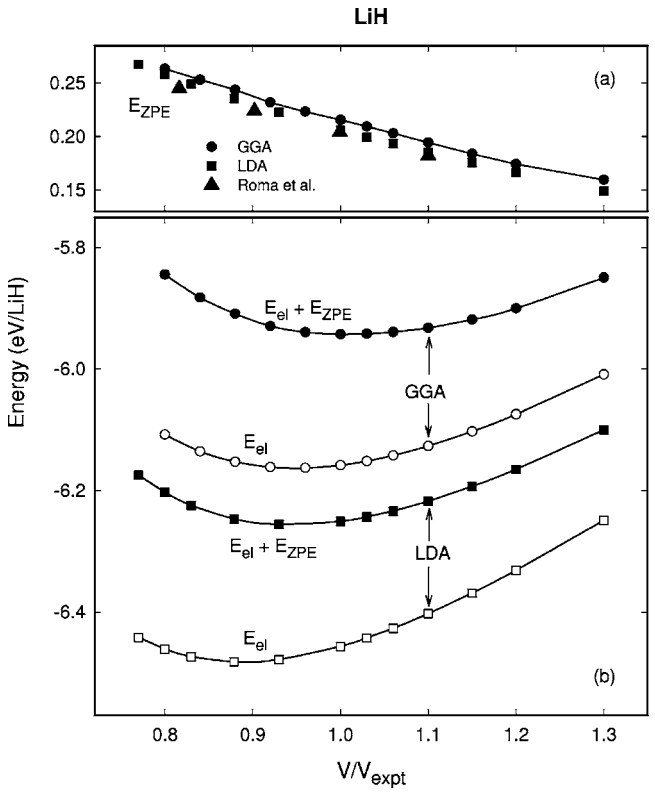

FIG. 2. (a) Zero point energy E_{ZPE} as a function of volume V calculated for LiH in the GGA (filled circles) and LDA (filled squares); filled triangles represent the results of Roma *et al.* (Ref. 27). (b) Electronic total energies E_{el} and $E_{el}+E_{ZPE}$ as functions of V calculated for LiH in the GGA (open and filled circles, respectively) and LDA (open and filled squares).

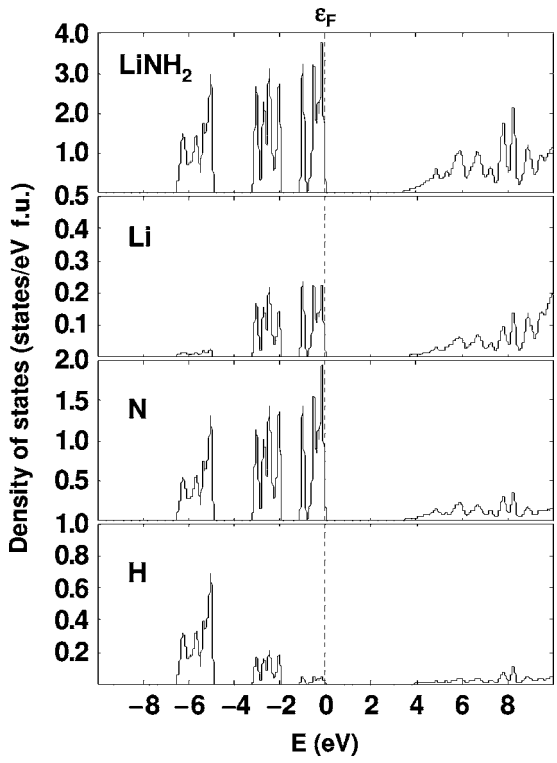

FIG. 3. Total and partial electronic densities of states calculated in the GGA for lithium amide, $LiNH_2$. The Fermi level ε_F is the energy zero.

B. Electronic densities of states

Figures 3 and 4 display total and site-projected GGA densities of states (DOS) for the amide, and Figs. 5 and 6 show analogous results for the imide. Both materials are insulators, a ~3 eV gap separating the valence and conduction bands in each. This is consistent with the interpretation of principally ionic bonding of Li^+ to $[NH_2]^-$ in the amide and to $[NH]^{-2}$ in the imide. Smaller 1.6 eV and 0.7 eV gaps occur in the occupied bands of the amide (top panel of Fig. 3), and a 1.4 eV gap is present in the occupied bands of the imide (top panel of Fig. 5); all are evidently structure induced. Orbital decomposition of the partial DOS for each element, using spheres of radii 1.1 Å, 0.85 Å, and 0.5 Å around the Li, N, and H sites, respectively, shows *s*-, *p*-, and much smaller *d*-like components in both compounds. Figure 4 (Fig. 6) displays the Li-*s*, Li-*p*, N-*s*, N-*p*, and H-*s* components for the amide (imide). In both materials H-*s* character is predominant, especially in the lowest occupied bands; the N-*p* component is most pronounced but distributed over all the filled states.

The occupied Li DOS is quite small (note the scale differences in Figs. 3–6), and integration inside the 1.1 Å Li spheres yields a rough estimate of $+0.7|e|$ net Li charge in the amide as well as the imide. Although there is some slight admixture of Li states with those derived from N and H, the binding between Li, essentially Li^+, and the N-H molecular complexes in both materials is most accurately described as primarily ionic. This characterization is firmly supported by examination of the electron localization function, ELF, originally developed for elucidating atomic shell structure and bond charge in molecular systems (definition and detailed description can be found in Refs. 29–31). The ELF is a position-dependent function having values confined to the $0 \leqslant \mathrm{ELF} \leqslant 1$ interval; ELF=0.5 corresponds to electron-gas-like pair probability. More recently the ELF has been used to investigate bonding in a variety of extended systems, including metals,[32] metal-ceramic interfaces,[33] earth materials,[34] and hydrogen storage materials.[35–37] Figure 7 (Fig. 8) displays ELF contours for the amide (imide). There are no significant values of ELF between Li and the N-H units, demonstrating the absence of any directional, covalent-type bonds. There is, however, quite clear ELF signature (i.e., ELF values exceeding 0.5) of the covalent bonding within the $[NH_2]^-$ and $[NH]^{-2}$ complexes. In the interest of completeness we note that the LiH DOS we obtain in either the GGA or LDA closely resembles that calculated by Smithson *et al.*[38] in the LDA; LiH is also an ionic insulator, with a similar gap of ~3 eV between the valence and conduction bands.

C. Amide and imide vibrational spectra

Figure 9 displays phonon densities of states derived from our calculations of the $LiNH_2$ and Li_2NH phonon dispersion relations. Analysis of the structures at 1478–1551 cm^{-1}, 3286–3306 cm^{-1}, and 3379–3386 cm^{-1} in the amide [Fig.

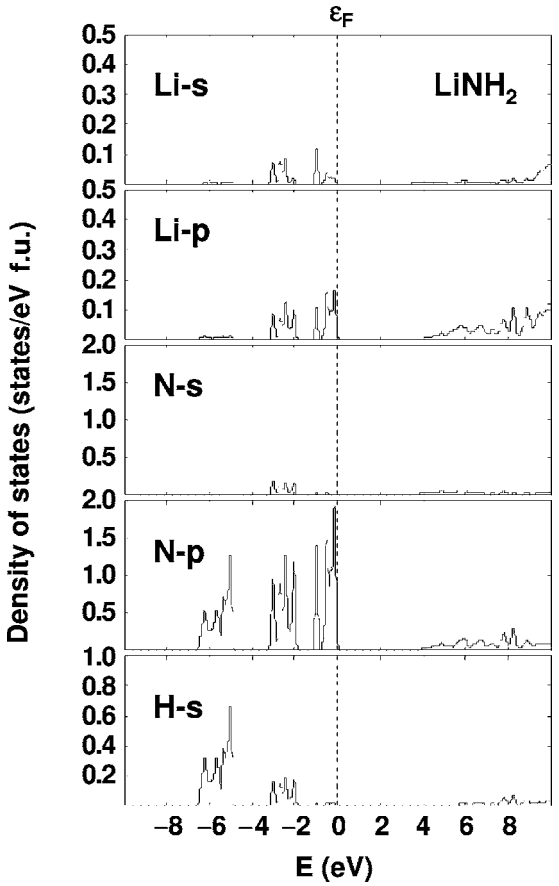

FIG. 4. Orbitally decomposed electronic densities of states calculated in the GGA for lithium amide, $LiNH_2$. The Fermi level ε_F is the energy zero.

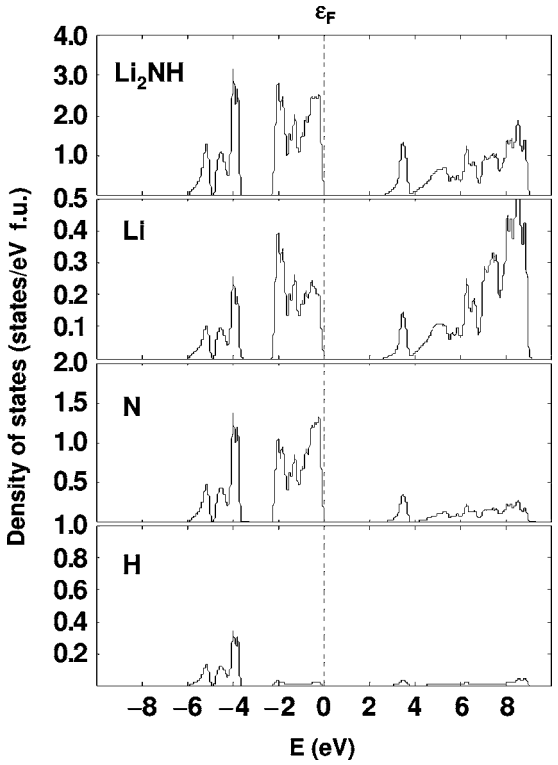

FIG. 5. Total and partial electronic densities of states calculated in the GGA for lithium imide, Li_2NH. The Fermi level ε_F is the energy zero.

9(a)] shows that they arise from H-N-H deformation, symmetric stretch, and asymmetric stretch modes of the NH_2 molecular units, respectively. From infrared (IR) and Raman experiments on solid NH_2 at 298 K Bohger *et al.*[39] determined that these modes occur at 1539–1561 cm^{-1}, 3258 cm^{-1}, and 3310–3315 cm^{-1}; Kojima and Kawai[40] observed the same energies for the stretch modes in IR spectra measured over the 2900–3400 cm^{-1} range. Bohger *et al.*[39] also obtained Raman spectra at 110 K and found the stretch modes to move to slightly higher energies of 3261 cm^{-1} and 3313–3326 cm^{-1}. In Li_2NH we find major structures corresponding to N-H stretch modes at 3199–3246 cm^{-1} and 3272 cm^{-1} [Fig. 9(b)]. While a gas phase diatomic molecule has a single vibrational mode, the two peaks here arise from the two slightly different N-H nearest-neighbor distances in the calculated GGA imide structure. Kojima and Kawai[40] report two IR bands in the vicinity of 3180 cm^{-1} and 3250 cm^{-1} for an imide sample prepared by thermally decomposing the amide. With a maximum departure of $\sim$60 cm^{-1}=0.007 eV, our calculated results for both materials are thus in very good accord with the available measurements. We infer that inclusion of LO-TO splittings in our phonon calculations would improve the agreement with experiment only marginally.

D. Enthalpies of formation

Assuming the ideal gas law for the molecules, the enthalpy $H=E+pV$ for each constituent at $T=0$ is

$$H_0 = E_{\mathrm{el}} + E_{\mathrm{ZPE}}, \tag{3}$$

where E_{el} is the electronic total energy and E_{ZPE} the zero point energy ($=\frac{1}{2}\Sigma_q \omega_q$ for the solids, $\frac{1}{2}\omega_0$ for H_2 and N_2, with ω the vibrational frequencies). The small molar volumes of the solids make pV negligible for them at $p=1$ bar. The $T=0$ enthalpy of formation ΔH_0, using the amide as an example, can then be written as the sum of electronic and ZPE components,

$$\begin{aligned}\Delta H_0(\mathrm{LiNH_2}) \equiv \Delta H_{\mathrm{el}} + \Delta H_{\mathrm{ZPE}} = &\left[E_{\mathrm{el}}(\mathrm{LiNH_2}) - E_{\mathrm{el}}(\mathrm{Li})\right. \\ &\left. - \tfrac{1}{2}E_{\mathrm{el}}(\mathrm{N_2}) - E_{\mathrm{el}}(\mathrm{H_2})\right] + \left[E_{\mathrm{ZPE}}(\mathrm{LiNH_2})\right. \\ &\left. - E_{\mathrm{ZPE}}(\mathrm{Li}) - \tfrac{1}{2}E_{\mathrm{ZPE}}(\mathrm{N_2}) - E_{\mathrm{ZPE}}(\mathrm{H_2})\right]. \end{aligned} \tag{4}$$

To obtain H at finite T we add the phonon energy (without the ZPE) $E_{\mathrm{ph}}=\Sigma_q \omega_q n(\omega_q)$, $n(\omega)=(e^{\omega/kT}-1)^{-1}$, to H_0 of each solid and the translational ($\frac{3}{2}kT$), rotational (kT), $pV=kT$, and vibrational $E_{\mathrm{vib}}=\omega_0 n(\omega_0)$ energy to H_0 of each molecule and write

$$\Delta H_T = \Delta H_0 + \delta\Delta H_T. \tag{5}$$

For the amide specifically we have

$$\begin{aligned}\delta\Delta H_T(\mathrm{LiNH_2}) = E_{\mathrm{ph}}(\mathrm{LiNH_2}) - E_{\mathrm{ph}}(\mathrm{Li}) - \tfrac{1}{2}\left[\tfrac{7}{2}kT + E_{\mathrm{vib}}(\mathrm{N_2})\right] \\ - \left[\tfrac{7}{2}kT + E_{\mathrm{vib}}(\mathrm{H_2})\right]. \end{aligned} \tag{6}$$

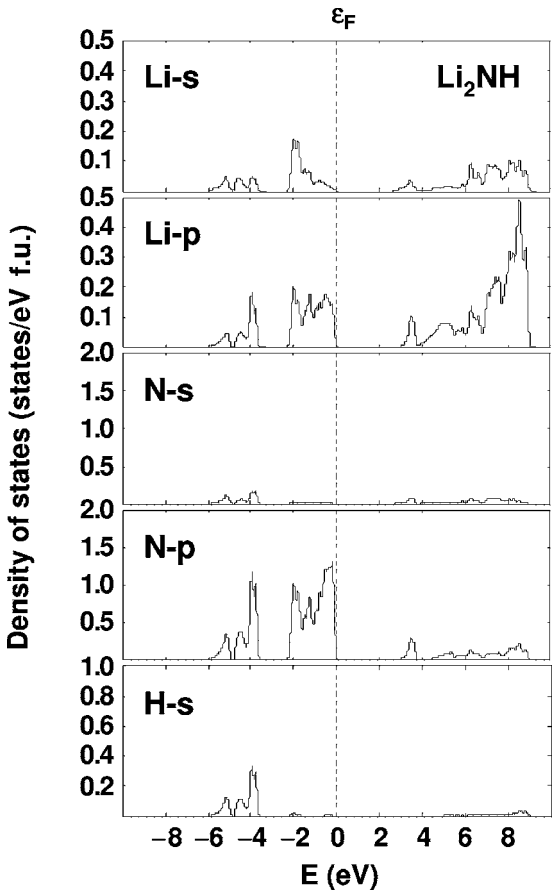

FIG. 6. Orbitally decomposed electronic densities of states calculated in the GGA for lithium imide, Li_2NH. The Fermi level ε_F is the energy zero.

Values of ΔH_0, ΔH_T at $T=298$ K, and their components as defined in Eqs. (4) and (5) are given in Table III along with available experimental data. The LDA yields values of ΔH_{el} that are more negative than those from the GGA, again underscoring the proclivity of the LDA to overbind; on a per mole-atom basis the differences are 9% ($LiNH_2$), 10% (Li_2NH), and 13% (LiH). Although ΔH_{el} is the largest component of ΔH_0 and ΔH_T, ΔH_{ZPE} is substantial and of opposite sign for all the compounds; for $LiNH_2$ it is 14% of $|\Delta H_0|$. The LDA values of ΔH_{ZPE} are larger than the GGA results over the narrow range of 0.6–0.9 kJ/mole atom (0.006–0.009 eV/atom); the corresponding percentage deviations vary from 3% ($LiNH_2$) to 15% (LiH) simply because of the small values of ΔH_{ZPE}. The E_{ph} and kT terms in Eq. (6) are on the order of 1 kJ/mole and the E_{vib} terms are insignificant at 298 K [we obtain $\omega_0(H_2)=4399$ cm^{-1} and $\omega_0(N_2)=2401$ cm^{-1}, in excellent comparison with the measured values[42] of 4405 cm^{-1} and 2360 cm^{-1}, respectively]. In Table III the $\delta\Delta H_{298}$ term correcting ΔH_0 to $T=298$ K is uniformly negative but only partially counterbalances ΔH_{ZPE} in the amide and imide. For $LiNH_2$ and LiH, ΔH_{298} in the GGA is in much better accord with the measurements than the LDA result. The heat of reaction

$$\Delta H_R \equiv \Delta H_{298}(Li_2NH) - \Delta H_{298}(LiNH_2) - \Delta H_{298}(LiH) \tag{7}$$

is $\Delta H_R=73.6$ kJ/mole in the GGA and 90.0 kJ/mole in the LDA, while the value obtained from the individual experimental ΔH_{298} entries in Table III is 45 kJ/mole. Chen *et al.*,[1] however, report $\Delta H_R=66$ kJ/mole from their direct measurement of H_2 absorption by Li_2NH. Since our GGA results for ΔH_R, $\Delta H_{298}(LiNH_2)$, and $\Delta H_{298}(LiH)$ agree well with experiment, we are led to infer that the experimental value for $\Delta H_{298}(Li_2NH)$ is inaccurate. A value of $\Delta H_{298}(Li_2NH)$

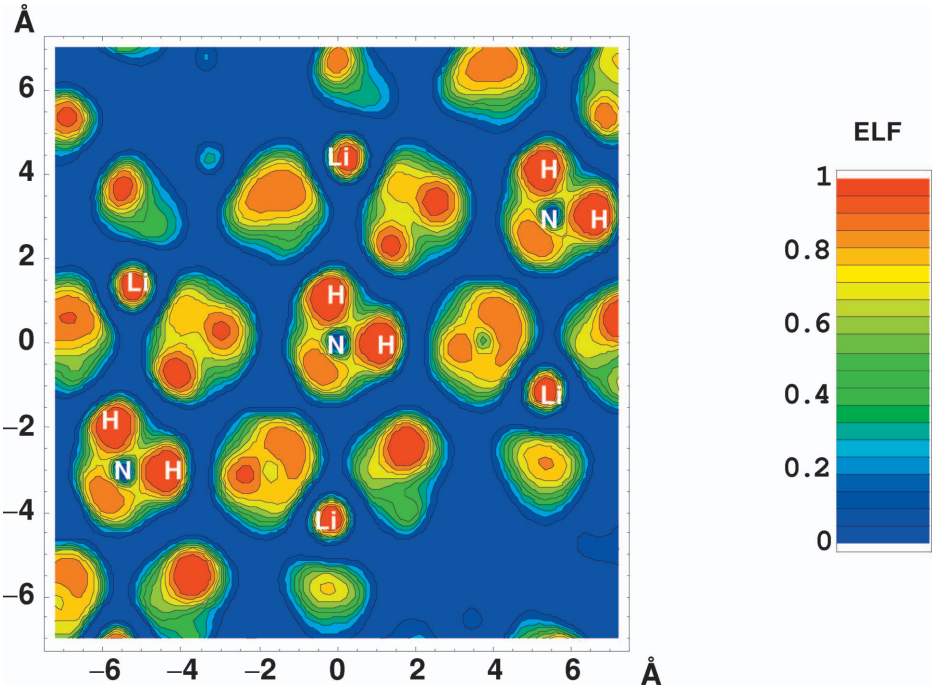

FIG. 7. (Color) Electron localization function calculated for $LiNH_2$ in a plane containing a $[NH_2]^-$ complex (center).

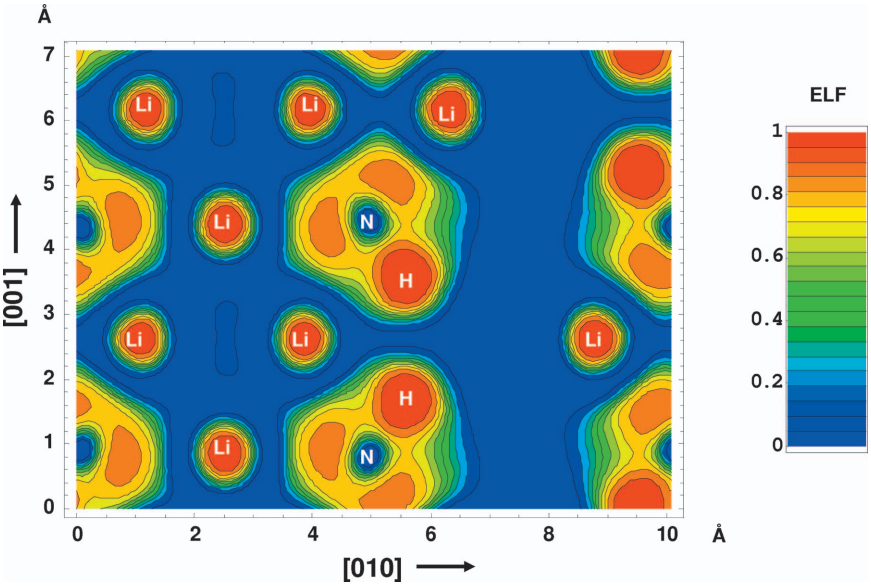

FIG. 8. (Color) Electron localization function calculated for Li_2NH in a (100) plane at $x=0.25$ (cf. Fig. 1).

nearer −200 kJ/mole, toward our calculated result, would afford much better consistency among our GGA results for ΔH_{298}, ΔH_R, and experiment.

We note that μ_{xc} has only small impact on the individual E_{ZPE} and E_{ph} terms appearing in ΔH. For $LiNH_2$ in the GGA (LDA) we find $E_{ZPE}=69.8$ (70.4), $E_{ph}=8.7$ (8.1); for Li_2NH in the GGA (LDA), $E_{ZPE}=46.7$ (47.9), $E_{ph}=9.5$ (9.0) (all energies in kJ/mole f.u.).

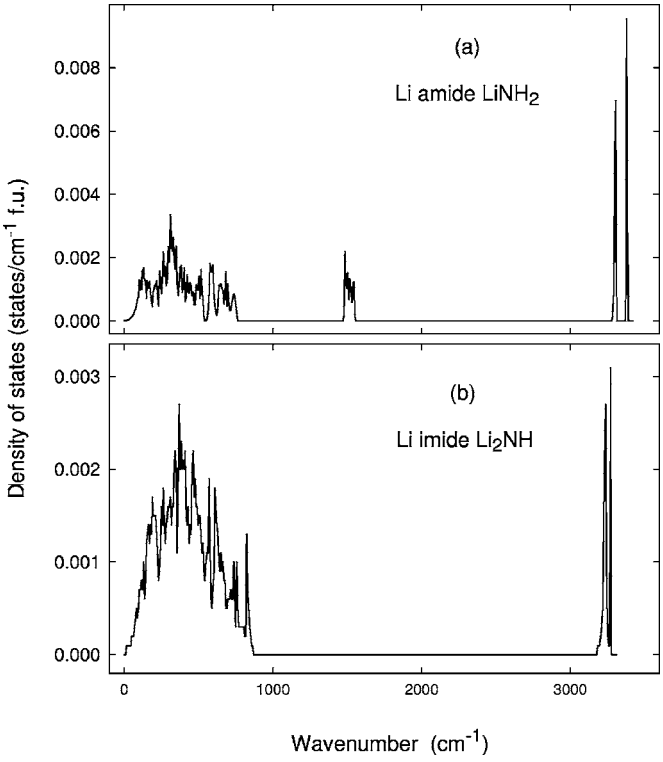

FIG. 9. Phonon densities of states calculated in the GGA for (a) Li amide, $LiNH_2$ [(2 2 1) supercells] and (b) Li imide, Li_2NH [(2 1 2) supercells].

IV. REMARKS

To summarize, we have provided a theoretical perspective on the recently identified hydrogen storage reaction (1) by calculating the electronic structure, vibrational spectra, and enthalpy of formation of each constituent using DFT in both the GGA and the LDA with PAW potentials. We find that $LiNH_2$, Li_2NH, and LiH are all ionic insulators. The phonon spectra calculated for $LiNH_2$ and Li_2NH agree very well with measurements of the N-H molecular modes in the solids. Our results unambiguously demonstrate that the GGA

TABLE III. Calculated $T=0$ and $T=298$ K enthalpies of formation, ΔH_0 and ΔH_{298}, respectively, and their components [cf. Eq. (4), Eq. (5)] for $LiNH_2$, LiH, and Li_2NH in both the LDA and GGA approximations. All values in kJ/mole f.u. (=0.010 364 eV/f.u.; f.u. ≡ formula unit).

	$LiNH_2$	LiH	Li_2NH
		LDA	
ΔH_{el}	−270.3	−105.5	−272.4
ΔH_{ZPE}	33.4	5.5	19.3
ΔH_0	−236.9	−100.0	−253.1
$\delta\Delta H_{298}$	−8.9	−5.0	−7.7
ΔH_{298}	−245.8	−105.0	−260.8
		GGA	
ΔH_{el}	−196.5	−83.9	−194.0
ΔH_{ZPE}	31.1	3.4	15.9
ΔH_0	−165.4	−80.5	−178.0
$\delta\Delta H_{298}$	−7.8	−4.1	−6.1
ΔH_{298}	−173.1	−84.6	−184.1
ΔH_0 expt		−85.548[b]	
ΔH_{298} expt	−176[a]	−90.625[b]	−222[a]

[a]Reference 1.
[b]Reference 41.

affords much better correspondence with experimental crystal structure information and with measurements of $\Delta H(LiNH_2)$, $\Delta H(LiH)$, and ΔH_R, leading us to suggest that $\Delta H(Li_2NH)$ warrants further experimental inquiry.

Technological prospects would be improved if $T \sim 280\,^{\circ}C$ at which the hydrogen plateau pressure for reaction (1) is $p \sim 1$ bar (Refs. 1 and 43) could be decreased. Elemental substitutions and additions to reduce ΔH_R are possibilities for doing so; work has already been reported on Mg substitution of Li (Refs. 43 and 44) and on replacement of $LiNH_2$ by $Mg(NH_2)_2$.[45] Additives also merit investigation. Encouraging in this regard is the fact that the $LiNH_2$ and Li_2NH structures are rather open (cf. Fig. 1, Fig. 7, and Fig. 8), each containing large voids that might accommodate additives.

ACKNOWLEDGMENTS

The authors are grateful to M. P. Balogh, T. W. Capehart, F. E. Pinkerton, P. Saxe, and J. J. Vajo for stimulating discussions.

[1] P. Chen, Z. Xiong, J. Luo, J. Lin, and K. L. Tan, Nature (London) **420**, 302 (2002).
[2] F. W. Dafert and R. Miklauz, Monatsch. Chem. **31**, 981 (1910).
[3] O. Ruff and H. Goerges, Chem. Ber. **44**, 502 (1911).
[4] P. Chen, Z. Xiong, J. Luo, J. Lin, and K. L. Tan, J. Phys. Chem. B **107**, 10967 (2003).
[5] T. Ichikawa, S. Isobe, N. Hanada, and H. Fujii, J. Alloys Compd. **365**, 271 (2004).
[6] G. P. Meisner, F. E. Pinkerton, M. S. Meyer, M. P. Balogh, and M. D. Kundrat, J. Alloys Compd. (to be published).
[7] K. H. J. Buschow, in *Handbook on the Physics and Chemistry of Rare Earths*, edited by K. A. Gschneidner, Jr. and L. Eyring (North-Holland, Amsterdam, 1984), Vol. 6, p. 1.
[8] W. Kohn and L. Sham, Phys. Rev. **140**, A1133 (1965).
[9] G. Kresse and J. Hafner, Phys. Rev. B **49**, 14251 (1994).
[10] G. Kresse and J. Furthmüller, Comput. Mater. Sci. **6**, 15 (1996).
[11] P. E. Blöchl, Phys. Rev. B **50**, 17953 (1994).
[12] D. M. Ceperley and B. J. Alder, Phys. Rev. Lett. **45**, 566 (1980).
[13] J. P. Perdew and Y. Wang, Phys. Rev. B **45**, 13244 (1992).
[14] J. P. Perdew, J. A. Chevary, S. H. Vosko, K. A. Jackson, M. R. Pederson, D. J. Singh, and C. Fiolhais, Phys. Rev. B **46**, 6671 (1992).
[15] P. Villars and L. D. Calvert, *Pearson's Handbook of Crystallographic Data for Intermetallic Phases*, 2nd ed. (ASM International, Materials Park, OH, 1991).
[16] M. Nagib and H. Jacobs, Atomkernenergie **21**, 275 (1973).
[17] D. K. Smith and H. R. Leider, J. Appl. Crystallogr. **1**, 246 (1968).
[18] *CRC Handbook of Chemistry and Physics*, 67th ed. (CRC Press, Boca Raton, FL, 1986), p. F-159.
[19] R. Juza and K. Opp, Z. Anorg. Allg. Chem. **266**, 325 (1951).
[20] T. Noritake, H. Nozaki, M. Aoki, S. Towata, G. Kitahara, Y. Nakamori, and S. Orimo, J. Alloys Compd. **393**, 264 (2005).
[21] K. Ohoyama, Y. Nakamori, S. Orimo, and K. Yamada, J. Phys. Soc. Jpn. **74**, 483 (2005).
[22] M. P. Balogh, C. Y. Jones, J. F. Herbst, L. G. Hector, Jr., and M. Kundrat (unpublished).
[23] D. R. Armstrong, P. G. Perkins, and G. T. Walker, J. Mol. Struct.: THEOCHEM **122**, 189 (1985).
[24] P. E. Blöchl, O. Jepsen, and O. K. Andersen, Phys. Rev. B **49**, 16223 (1994).
[25] J. Lazewski, P. T. Jochym, and K. Parlinski, J. Chem. Phys. **117**, 2726 (2002).
[26] K. Parlinski, J. Alloys Compd. **328**, 97 (2001).
[27] G. Roma, C. M. Bertoni, and S. Baroni, Solid State Commun. **98**, 203 (1996).
[28] O. L. Anderson, *Equations of State of Solids for Geophysics and Ceramic Science* (Oxford University Press, New York, 1995).
[29] A. D. Becke and K. E. Edgecombe, J. Chem. Phys. **92**, 5397 (1990).
[30] B. Silvi and A. Savin, Nature (London) **371**, 683 (1994).
[31] A. Savin, R. Nesper, S. Wengert, and T. F. Fässler, Angew. Chem., Int. Ed. Engl. **36**, 1808 (1997).
[32] R. Rousseau and D. Marx, Chem.-Eur. J. **6**, 2982 (2000).
[33] D. J. Siegel, L. G. Hector, Jr., and J. B. Adams, Phys. Rev. B **65**, 085415 (2002).
[34] G. V. Gibbs, D. F. Cox, N. L. Ross, T. D. Crawford, J. B. Burt, and K. M. Rosso, Phys. Chem. Miner. **32**, 208 (2005).
[35] P. Ravindran, P. Vajeeston, H. Fjellvåg, and A. Kjekshus, Comput. Mater. Sci. **30**, 349 (2004).
[36] L. G. Hector, Jr., J. F. Herbst, and T. W. Capehart, J. Alloys Compd. **353**, 74 (2003).
[37] L. G. Hector, Jr. and J. F. Herbst, J. Alloys Compd. **379**, 41 (2004).
[38] H. Smithson, C. A. Marianetti, D. Morgan, A. Van der Ven, A. Predith, and G. Ceder, Phys. Rev. B **66**, 144107 (2002).
[39] J.-P. Bohger, R. R. Essmann, and H. Jacobs, J. Mol. Struct. **348**, 325 (1995).
[40] Y. Kojima and Y. Kawai, J. Alloys Compd. **395**, 236 (2005).
[41] J. Phys. Chem. Ref. Data Monogr. No. 9 (American Chemical Society, Woodbury, New York, 1998), p. 1274.
[42] G. Herzberg, *Molecular Spectra and Molecular Structure, I. Diatomic Molecules* (Prentice-Hall, New York, 1939).
[43] W. Luo, J. Alloys Compd. **381**, 284 (2004).
[44] Y. Nakamori and S. Orimo, J. Alloys Compd. **370**, 271 (2004).
[45] H. Y. Leng, T. Ichikawa, S. Hino, N. Hanada, S. Isobe, and H. Fujii, J. Phys. Chem. B **108**, 8763 (2004).